Multiphase electropatterning of cells and biomaterials†

Dirk R. Albrecht,‡[a] Gregory H. Underhill,[a] Avital Mendelson§[a] and Sangeeta N. Bhatia*[ab]

Received 29th January 2007, Accepted 27th March 2007
First published as an Advance Article on the web 18th April 2007
DOI: 10.1039/b701306j

Tissues formed by cells encapsulated in hydrogels have uses in biotechnology, cell-based assays, and tissue engineering. We have previously presented a 3D micropatterning technique that rapidly localizes live cells within hydrogels using dielectrophoretic (DEP) forces, and have demonstrated the ability to modulate tissue function through the control of microscale cell architecture. A limitation of this method is the requirement that a single biomaterial must simultaneously harbor biological properties that support cell survival and function *and* material properties that permit efficient dielectrophoretic patterning. Here, we resolve this issue by forming multiphase tissues consisting of microscale tissue sub-units in a 'local phase' biomaterial, which, in turn, are organized by DEP forces in a separate, mechanically supportive 'bulk phase' material. We first define the effects of medium conductivity on the speed and quality of DEP cell patterning. As a case study, we then produce multiphase tissues with microscale architecture that combine high local hydrogel conductivity for enhanced survival of sensitive liver progenitor cells with low bulk conductivity required for efficient DEP micropatterning. This approach enables an expanded range of studies examining the influence of 3D cellular architecture on diverse cell types, and in the future may improve the biological function of inhomogeneous tissues assembled from a variety of modular tissue sub-units.

Introduction

Microscale technologies have emerged as powerful tools to control the cellular microenvironment for cell-based assays and engineered tissues.[1,2] Such methods allow precise positioning of cells in order to define interactions between neighboring cells and to spatially localize matrix molecules and soluble factors. Because cells integrate and respond to these microenvironmental signals, micropatterning methods have been utilized, for example, to stabilize cell phenotype *in vitro*[3] and to direct differentiation of stem cells.[4] Recently, we have developed a method for the patterning of living cells in 3 dimensions (3D) as a tool to define cellular microarchitecture.[5] The technique uses dielectrophoretic (DEP) forces to localize live cells within a liquid precursor solution to microfabricated electrodes. Subsequent crosslinking of the hydrogel then traps microorganized cells for long-term culture. By moving all cells in parallel, this electrokinetic method can be scaled to large cellular constructs without increasing fabrication time, unlike serial patterning methods.[6,7]

DEP forces most efficiently pattern cells within low-viscosity, low-conductivity biomaterials.[8] We have previously reported DEP cell patterning within 15% PEG and 1% agarose hydrogels, with precursor solution conductivity below 21 mS m^{-1} and viscosity below 7 cP. These materials promoted cell survival and differentiated function of several cell types, such as bovine chondrocytes, murine fibroblasts, and murine hepatocyte/fibroblast co-cultures, in some cases up to several weeks.[5,9] However, many conventional cell culture biomaterials, such as collagen, alginate, and Matrigel™, are less suitable for use with DEP electropatterning because they are more conductive, more viscous, or difficult to gel in a closed chamber. In many cases, polymer precursors may be modified to meet some of these requirements. For example, enzymatic or irradiation treatments may reduce polymer molecular weight and thereby the viscosity of precursor solutions.[10] To permit remote triggering of gelation within the closed DEP patterning apparatus, many biomaterials can be rendered photocrosslinkable by acrylation,[11] and ion-sensitive hydrogels may be gelled *via* release of caged or liposome-sequestered ions.[12] The conductivity of the precursor solution, however, is difficult to reduce due to inherent material properties often required for gelation, notably charged moieties. DEP cell localization can occur in highly conductive media;[13] however, under these conditions, it has not been successfully scaled to large electrode arrays due to weakened DEP forces, strengthened non-DEP electrokinetic forces (*e.g.* electroosmotic flow), emergence of local thermal and ionic gradients,[8,14,15] and decreased chamber impedance which necessitates more sophisticated electrical equipment.

In this paper, we present an alternative strategy to permit the 3D micropatterning of cells surrounded by any biomaterial. Rather than positioning individual cells within a single hydrogel as we have previously reported, we demonstrate here

[a]*Harvard–M.I.T. Division of Health Sciences and Technology/Electrical Engineering and Computer Science, Massachusetts Institute of Technology, 77 Massachusetts Ave., E19-502D, Cambridge, MA, USA*
[b]*Division of Medicine, Brigham and Women's Hospital, Boston, MA, USA. E-mail: sbhatia@mit.edu; Fax: +1 617 324-0740; Tel: +1 617 324-0221*

† This paper is part of a special issue 'Cell and Tissue Engineering in Microsystems' with guest editors Sangeeta Bhatia (MIT) and Christopher Chen (University of Pennsylvania).

‡ Present address: The Rockefeller University, 1230 York Avenue, Box 204, New York, NY, USA
§ Present address: Cornell University, Ithaca, NY, USA

the ability to electropattern pre-formed cell-laden hydrogel microstructures, or microgels, composed of a "local-phase" biomaterial, within a distinct "bulk phase" (Fig. 1). The bulk-phase material is subject to conductivity and viscosity limitations to enable DEP patterning whereas the "local-phase" microgel material is not. We first determine practical limits to bulk-phase conductivity by exploring the effects of medium conductivity on the speed and quality of DEP cell patterning. Next, we demonstrate that the survival of a bipotential mouse embryonic liver (BMEL) progenitor cell type is indeed improved in some higher conductivity materials such as alginate over polyethylene glycol. We then demonstrate effective multiphase DEP patterning of conductive, cell-free, alginate microgels within a less conductive bulk phase, agarose. Finally, BMEL cells are encapsulated in the conductive microgels and are shown to pattern efficiently by DEP within a low-conductivity hydrogel. The technology represents an opportunity to fabricate hydrogel tissues with microscale organization in spite of the difficulty in identifying a single material that would both support BMEL survival and enable dielectrophoretic patterning. The fabrication of multiphase tissues by combining cell encapsulation and dielectrophoretic patterning represents a generalizable strategy to broaden the utility of electropatterning of cells in tissues.

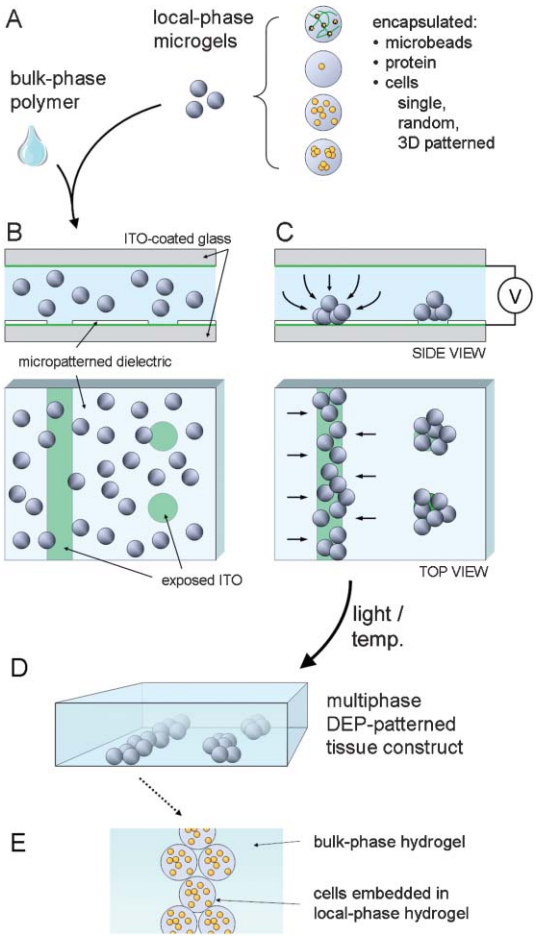

Fig. 1 Fabrication of multiphase DEP-patterned tissue constructs. (A) Hydrogel microstructures, or 'microgels,' are first prepared by encapsulation or molding techniques and may contain a variety of bioactive materials and/or cells. (B) Local-phase microgels are mixed with the bulk-phase polymer precursor solution and introduced into the transparent DEP patterning chamber. On the lower glass chamber slide, a micropatterned dielectric layer masks the conductive indium tin oxide (ITO) to form electrodes. (C) Upon application of the ac chamber bias, microgels move *via* positive DEP forces (arrows) to regions of high electric field strength directly above the exposed ITO. (D) The bulk-phase polymer is then crosslinked by exposure to light or a change in temperature, thereby trapping patterned microgels. The multiphase tissue construct can then be removed from the chamber and cultured. (E) Embedded cells are directly surrounded by a local-phase biomaterial, whereas the entire construct is supported by the bulk-phase hydrogel.

Materials and methods

Cell culture

Swiss 3T3 murine fibroblasts (American Type Culture Collection, Manassas, VA) were cultured in 150 cm^2 flasks (Fisher, Springfield, NJ) in Dulbecco's Modified Eagle Medium (DMEM; Gibco, Grand Island, NY) supplemented with 10% bovine calf serum, 100 μg mL^{-1} penicillin, and 100 μg mL^{-1} streptomycin and incubated in 5% CO_2 at 37 °C. The BMEL cell line, 9A1, was provided by Dr. Mary Weiss (Institut Pasteur) and cultured as described previously.[16,17] In brief, cells were maintained in collagen-coated flasks in RPMI 1640 medium with glutamax (Invitrogen), containing 30 ng mL^{-1} human IGF-II (Peprotech), 50 ng mL^{-1} human EGF (Peprotech), and 10 μg mL^{-1} recombinant human insulin (Invitrogen) and passaged every 2–4 days. Prior to patterning experiments, cells were released from tissue culture flasks into suspension using a solution of 0.25% trypsin with 1 mM EDTA (Gibco).

DEP patterning apparatus

A transparent chamber was fabricated to establish a non-uniform electric field required for dielectrophoretic patterning of cells or hydrogel microparticles, similar to previous reports.[5,18] Briefly, indium tin oxide (ITO)-coated conductive glass slides (Delta Technologies CB-40IN or CB-50IN) were separated by a thin silicone gasket to enclose a 10 × 20 × 0.1 mm^3 volume. To selectively expose conductive "electrodes" on one ITO surface, a 1.8 μm thick insulative epoxy layer (SU-8, Microchem) was patterned photolithographically through an emulsion mask printed at 5080 dpi (PageWorks). The epoxy film was cured at 185 °C for 1 hr to complete crosslinking and immersed in distilled water overnight to ensure biocompatibility. Assembled chambers were sterilized with 70% ethanol and treated with Pluronic F108 (1%, BASF) for 10–20 min to resist protein adsorption and decrease cell or particle adhesion. A larger chamber was used for hydrogel microsphere patterning, as described below.

Hydrogel precursor conductivity and viscosity

Electrical conductivity was measured with a low cell volume, flow-through probe (Microelectrodes, Inc. #16–900) and a Consort C535 meter. Viscosity measurements were obtained with a Zeitfuchs cross-arm viscometer. All data were obtained

at 25 °C, or at a temperature appropriate for the liquid phase of thermally gelling polymers (4 °C or 37 °C).

Conductivity analysis

To analyze the effect of medium conductivity on cell patterning, fibroblast suspensions (10×10^6 mL^{-1}) were prepared in an isoosmotic, low-conductivity buffer (LCB: 10 mM HEPES, 0.1 mM $CaCl_2$, 59 mM D-glucose and 236 mM sucrose, pH 7.35) supplemented with 0–10% fetal bovine serum (FBS). Electrical conductivity ranged from 21.4 mS m^{-1} (LCB + 0% FBS) to 135 mS m^{-1} (LCB + 10% FBS). Polystyrene microbeads (10 μm, Bangs Labs) were added to the cell suspension to verify the presence of the electric field, as DEP-induced forces exerted on them are insensitive to medium conductivity. After flushing the chamber with >10 volumes of cell-free buffer, the cell suspension was drawn into the chamber through fluidic ports (NanoPort, Upchurch) and a syringe. A 2.3 V_{rms}, 3 MHz sinusoidal ac chamber bias was applied *via* a function generator (Agilent 33120A), and monitored by an oscilloscope (Tektronix TDS2014) connected in parallel. Images of cell motion were captured using a Nikon Ellipse TE200 inverted microscope with Hoffmann optics and analyzed using MetaMorph software. Image stacks were background subtracted and subjected to manual thresholding for segmentation to compute area and perimeter of patterned cell clusters (as a measure of cluster compactness). As a measure of DEP patterning progress, the average spacing between cells or clusters was calculated for each video frame as 4 times the mean Euclidean distance of non-cell pixels (since area-averaged Euclidean distance of regions between parallel lines is equal to one fourth the spacing between lines).

Hydrogel encapsulation of BMEL cells

For hydrogel encapsulation, dispersed BMEL cells were re-suspended at a 2× concentration in BMEL cell culture medium. The cell suspension was then added 1 : 1 to a 2× polymer solution for a final cell concentration of 10×10^6 BMEL cells mL^{-1}. Poly(ethylene glycol) (PEG) polymer solutions contained a final concentration of 10% w/v 3.4 kDa PEG-diacrylate (PEG-DA, Nektar Therapeutics, Huntsville, AL) and 0.05% w/v Irgacure 2959 photoinitiator (I-2959, Ciba). PEG hydrogels, 250 μm or 500 μm thick and 1.1 cm in diameter, were prepared on 18 mm cover glass circles (Fisher Scientific) using a polymerization apparatus previously described.[19] The photosensitive PEG hydrogel was crosslinked by exposure to 320–390 nm UV light (10 mW cm^{-2}) for 70 s with an EXFO Lite UV spot curing system equipped with a collimating lens (EXFO, Mississuaga, ON, Canada). Alginate solutions contained a final concentration of 2% Protanal 10/60 LF (FMC Biopolymer) in culture medium, with or without 0.2 mg mL^{-1} rat tail collagen, and were gelled by the addition of 8 μl droplets into 102 mM $CaCl_2$. After 5 min, the approximately 2.5 mm diameter spheroidal hydrogels were fully gelled and contained a uniform distribution of encapsulated cells. Hydrogels were subsequently washed with PBS, followed by culture medium, and then cultured in BMEL cell culture medium with media changes every other day.

Assessment of encapsulated BMEL viability

Cell viability was examined by labeling with calcein AM (5 μg mL^{-1}) and ethidium homodimer (2.5 μg mL^{-1}) (live/dead) fluorescent stains (Molecular Probes). Images were acquired using a Nikon Eclipse TE200 inverted fluorescence microscope and CoolSnap-HQ Digital CCD Camera. Viability of encapsulated cells was quantified using the dimethylthiazol–diphenyltetrazolium bromide (MTT) assay. Replicate hydrogels for each condition were incubated in phenol red-free DMEM (Gibco) containing 0.5 mg mL^{-1} MTT (Sigma) for 1.5 h at 37 °C. The resulting precipitate was then solubilized by the addition of 50% isopropanol–50% DMSO and the absorbance at 570 nm (minus background absorbance at 660 nm) was quantified. Absorbance measures were normalized to day 0 values.

Alginate microsphere production

To form calcium-crosslinked alginate microspheres, the alginate solution (2% Protanal LF 10/60 in 0.85% NaCl) was extruded through a 23 gauge needle at a constant rate of 0.05 mL min^{-1} using a syringe pump. Alginate solutions further contained either 10×10^6 BMEL cells mL^{-1}, or 1.9×10^8 mL^{-1} Flash Red-labeled polystyrene microbeads (1 μm diameter, Bangs Laboratories) and 0.2 mg mL^{-1} Oregon Green® 488-conjugated human collagen type IV (Invitrogen). Alginate droplets were crosslinked upon contact with a gently agitated 102 mM $CaCl_2$ precipitation solution and were washed after 5–10 min incubation. An air jet of 24 L min^{-1} surrounding the needle provided a droplet size of <200 μm, and alginate microspheres were further filtered using a 100 μm Cell Strainer (Falcon) to remove larger aggregates. Some alginate microspheres were then coated with a poly-lysine layer to provide mechanical stability and a diffusion barrier, as previously described.[20] In brief, alginate microspheres were sequentially treated with the following solutions: 1.1%, 0.55%, and 0.28% $CaCl_2$; 0.1% CHES (Sigma) in 0.85% NaCl; 0.05% poly-L-lysine (PLL, 15–30 kDa, Sigma) for 6 min; 0.5% PEG (4 kDa) in 0.45% NaCl for 10 min; 0.1% CHES; 1.1% $CaCl_2$; 2× with 0.85% NaCl; 0.2% alginate in 0.85% NaCl for 4 min; and finally 2 washes with cell culture medium. The alginate–PLL–alginate (APA) and uncoated alginate microspheres were prepared fresh, maintained in BMEL culture medium, and used within 12 h.

DEP patterning of alginate microspheres in agarose hydrogels

Uncoated alginate or APA microspheres were washed twice in low-conductivity buffer and mixed 1 : 1 with a 2% agarose solution (ultralow gelling temperature, Type IX-A, Sigma A2576) in low-conductivity buffer. Solutions were kept at 37 °C to maintain a liquid state prior to and during patterning. The alginate microspheres in 1% agarose were drawn into a DEP patterning apparatus with a larger $20 \times 20 \times 0.25$ mm^3 chamber volume to accommodate the ~100 μm diameter microgels. This apparatus was energized with a 12–14 V_{rms}, 1 MHz ac bias using a Hewlett-Packard 8647A signal source coupled with a broadband radiofrequency amplifier (EIN 420LA). After patterning, the syringe valve was closed to

prevent any flow in the chamber, and the apparatus was submerged in an ice–water bath for 5 min. Next, the apparatus was warmed to room temperature and opened. The gelled agarose slab containing patterned alginate microspheres was transferred to saline or BMEL culture medium and viewed in brightfield and fluorescence microscopy. BMEL-containing hydrogels were assessed for cell viability as described above. Some agarose gels containing embedded alginate microspheres were immersed in a dissolution buffer (55 mM sodium citrate) to dissolve the alginate gel *via* chelation of the crosslinking calcium ions.

Results and discussion

Multiphase patterning approach

The multiphase strategy spatially divides the cell encapsulation biomaterial into a local phase, immediately surrounding the cell and tailored to best support cell survival and function, and a bulk phase, in which patterning occurs *via* DEP forces (Fig. 1). Local-phase microgels containing embedded cells or other constituents are first prepared by standard microencapsulation techniques, then mixed with the bulk-phase hydrogel precursor solution (Fig. 1A). This mixture is drawn into the patterning apparatus (Fig. 1B) and the ac chamber bias is applied to elicit DEP forces that propel microgels toward the microfabricated electrodes (Fig. 1C). Upon bulk-phase gelation *via* a change in temperature or exposure to light, microgels become fixed in the prescribed pattern and the entire multiphase hydrogel construct can be removed from the chamber and cultured (Fig. 1D). We first determined conductivity limits for the bulk phase, and then demonstrated fabrication of multiphase tissues that locally surround cells with a conductive material, which afforded improved cell survival.

Effect of medium conductivity on positive DEP cell patterning

Relative DEP force is specified by the real portion of the Clausius–Mossotti factor, a complex scaling term that represents the relative polarizability between the motile particle (cell or microgel) and the medium.[14,15] Fig. 2 shows relative DEP force calculated for typical mammalian cells and alginate microbeads suspended in media of varying conductivity. DEP force declines with increasing conductivity for both cells and alginate beads, particularly in the 1–10 MHz frequency range typical for cell patterning. For example, only one-half the DEP force is predicted for cells in media equivalent to 1/10 of physiological saline ($\sim$135 mS m^{-1}) compared with cell in a low-conductivity buffer (LCB, 21 mS m^{-1}).

To explore this experimentally, we organized fibroblasts into arrays of cell clusters in media of increasing conductivity and monitored electropatterning speed and steady-state pattern quality. Positive DEP forces, evident by cell motion toward the hexagonal array of electrodes spaced 100 μm apart, were apparent in media containing LCB and up to 10% FBS (135 mS m^{-1}) (Fig. 3A). As predicted, patterning slowed with increasing conductivity (Fig. 3C). However, pattern quality (as measured by compactness of clusters containing equivalent cell number and mean distance between them) also decreased in more conductive media (Fig. 3C,D). Surprisingly, even a

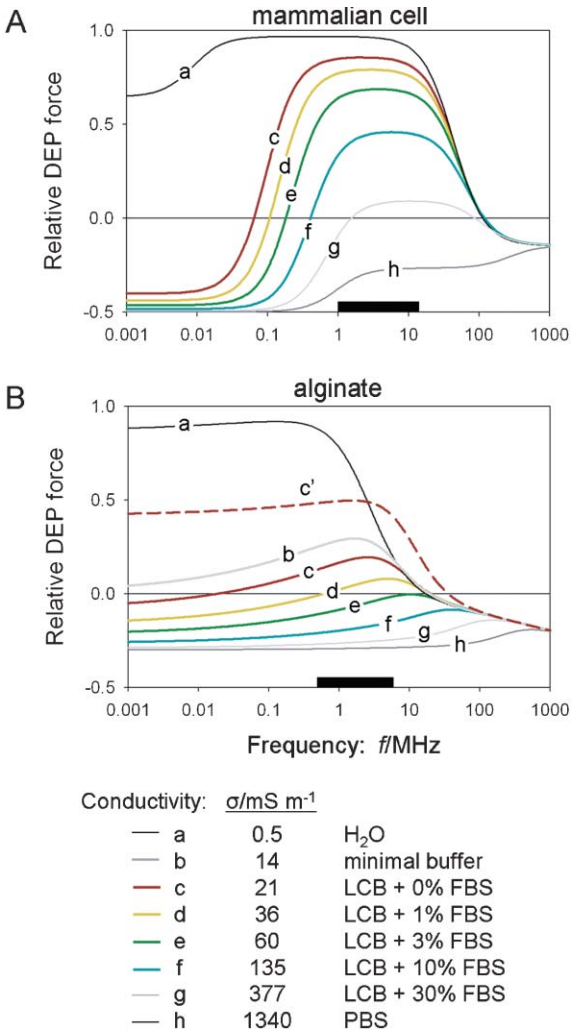

Fig. 2 Relative DEP force decreases with increasing medium conductivity for both mammalian cells (**A**) and alginate microgels (**B**). Maximum positive DEP force in low-conductivity buffer (LCB) occurs in the frequency range of $\sim$1–10 MHz for both cells and alginate microgels. Increasing the conductivity of alginate, *e.g.* by copolymerizing with matrix molecules, further increases relative DEP force in this frequency range (broken line). Calculations are based on models and electrical properties for white blood cells[29] and 2% calcium alginate beads,[30] adding 50 mS m^{-1} to internal alginate conductivity to simulate addition of conductive molecules. LCB, low-conductivity buffer; FBS, fetal bovine serum; PBS, phosphate-buffered saline.

very small (1%) addition of conductive FBS produced a significant 60% increase in cluster area. Cell cluster shape is dictated by the magnitude of DEP force relative to other electric field-mediated forces, such as interparticle attraction–repulsion and electroosmotic forces. At low conductivity, strong DEP forces pull cells into a 3D cluster shape whereas even minor decreases in DEP force in higher conductivity media result in flat, 2D cell clusters (Fig. 3B). These results suggest that efficient DEP patterning requires a bulk-phase solution conductivity less than approximately 40 mS m^{-1} and ideally 20 mS m^{-1} or below. PEG-based hydrogels and agarose are ideal by this standard and have been used

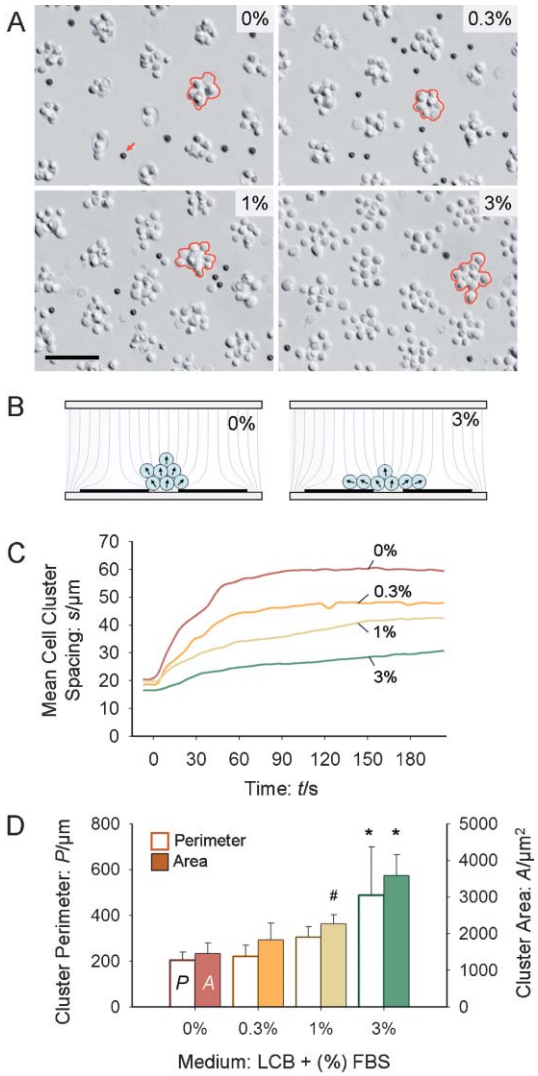

Fig. 3 Positive DEP patterning is sensitive to electrical conductivity of the bulk-phase hydrogel. (A) Fibroblasts are shown electropatterned in a hexagonal array in media of increasing conductivity, by the addition of indicated concentrations of fetal bovine serum (FBS) to low-conductivity buffer (LCB). Conductivity values are listed in Fig. 2. Cell clusters averaged 10 cells each for all conditions. Polystyrene microbeads (dark spots, see arrow) move away from electrodes in a conductivity-insensitive manner and verify the applied electric field. Scale bar, 100 μm. (B) Cell clusters appear smaller in lower conductivity media because cells form 3D, spherical clusters as DEP forces overcome interparticle repulsion between adjacent cells oriented perpendicular to their dipoles (arrows). Clusters in higher conductivity media are flat with most cells oriented parallel with their dipoles. (C) The evolution of cell patterning over time was quantified as the average distance between cells or cell clusters, using image segmentation of video similar to (A). (D) Cluster compactness is reflected by cluster perimeter (red outlines in A) and area. Data are mean ± SD (n = 6–10) and statistical significance is indicated by (*) compared with 0–1% FBS, and by (#) compared with 0% FBS, with $p < 0.001$ (t-test).

successfully for cell electropatterning, but many commonly-utilized cell encapsulating biomaterials have higher conductivity and are unsuitable as bulk-phase hydrogels for DEP cell patterning (Table 1).

Survival of hydrogel encapsulated BMEL cells

Low-conductivity biomaterials lack ions and potentially essential proteins and soluble factors, which together impart a relatively high conductivity to standard culture media ($\sim$1400 mS m^{-1}). Thus, cells encapsulated in these materials may suffer decreased survival or otherwise function poorly. Nonetheless, many cell types have been successfully encapsulated in low-conductivity PEG and agarose, such as fibroblasts and chondrocytes, and cultured for up to several weeks while maintaining differentiated cell functions.[5] One mitigating factor in these examples is the relatively short (<1 hr) exposure of cells to low conductivity buffer, which was quickly replaced with full culture medium. Some cells, however, may perform poorly even with short exposure to suboptimal media.

We examined the survival of an undifferentiated liver progenitor cell line (BMEL) embedded within selected low- and high-conductivity biomaterials. BMEL cells were encapsulated in low-conductivity PEG hydrogels using photopolymerization parameters previously selected to minimize toxicity.[9] Viability, as determined by calcein AM/ethidium homodimer (live/dead) staining, was high immediately after encapsulation but declined markedly in 10% PEG hydrogels by day 2 despite culture in complete medium (Fig. 4A). In contrast, BMEL cells encapsulated in conductive 2% alginate gels maintained high viability at day 2 (Fig. 4B). The effect of encapsulation biomaterial on BMEL cell survival was verified by quantitative MTT staining, a measure of mitochondrial activity. Consistent with the fluorescent viability assay, BMEL cell survival in 10% PEG hydrogels diminished two-fold by day 2, but did not decrease in 2% alginate (Fig. 4C). Coencapsulation of BMELs in alginate and 0.2 mg mL^{-1} collagen also maintained cell survival and further provided extracellular matrix for cell attachment, a common requirement for adhesion-dependent cells. Enhanced viability in the alginate gel may reflect increased nutrient transport, as the pore size is up to 10-fold greater[21] compared with the PEG gel,[22] and the inability of cells to attach to unmodified PEG. These results illustrate the sensitivity of BMEL cells to the encapsulating biomaterial, and are consistent with the more general use of conductive hydrogels for cell encapsulation.

Multiphase DEP-patterned hydrogel constructs

Because positive DEP forces require the polarizability (*i.e.*, at high frequency, the conductivity) of the moving particle to be greater than the surrounding medium, the local-phase hydrogel is ideally highly conductive. This enables the use of virtually any biomaterial, even neutral polymers with inherently low conductivity, which may be rendered conductive by the coencapsulation of charged molecules or the chemical addition of charged groups. For example, 2% calcium alginate microgels are relatively conductive ($\sim$200 mS m^{-1}) and pattern by positive DEP in the frequency range 1–10 MHz (Fig. 2B). Any further increase in alginate conductivity, such as by coencapsulation or coating with charged polymers (*e.g.*, poly-L-lysine), would strengthen patterning force (Fig. 2B, broken line).

To demonstrate the multiphase micropatterning concept, we selected 2% alginate as the conductive, local-phase hydrogel

Table 1 Properties of selected common cell encapsulation hydrogels. PEG and agarose are ideal hydrogels for DEP patterning, whereas many other biomaterials commonly used for cell encapsulation are either too conductive, too viscous, or are difficult to gel in a closed chamber

Hydrogel	Concentration (typical for cell encapsulation)	Conductivity (dissolved in LCB, pH 7.4)	Viscosity (at prepolymer temp.)		Gelation Mechanism
PEG-DA (3.4 kDa)	10%–20%	15 mS m^{-1}	2.4 cP (10%) 3.3 cP (15%) 5.4 cP (20%)	25 °C	light
Agarose (Type IX-A)	1%	20 mS m^{-1}	7 cP	37 °C	temp.
Alginate (low viscosity)	1%–2%	200 mS m^{-1}	21.4 cP (1.2%)	25 °C	ionic
Collagen I (rat tail)	0.9 mg mL^{-1}	1380 mS m^{-1} [a]	4.3 cP	4 °C	pH/temp.
Matrigel™	10–12 mg mL^{-1}	1380 mS m^{-1} [a]	15.2 cP	4 °C	temp.

[a] Collagen and Matrigel™ were tested as supplied, as liquid solutions in DMEM. Collagen is soluble in 0.1 M acetic acid, pH 3 (~65 mS m^{-1}), although gelation performance in low conductivity media is unclear.

that supported BMEL cell survival (Fig. 4), and 1% agarose as a low-conductivity, low-viscosity, and thermally-gelling bulk-phase material compatible with rapid localization *via* DEP forces. Both the high viscosity of alginate and its gelation by addition of chelating ions suggest that alginate is unsuitable as the bulk-phase material for direct DEP cell patterning. We first prepared 30–70 μm diameter calcium alginate microspheres with encapsulated fluorescent collagen IV and fluorescent 1 μm polystyrene microbeads, in order to visualize microgel patterning and as an example of bioactive but acellular constituents. After several minutes of exposure to the electric field, alginate microgels localized in the molten agarose solution with good fidelity to parallel line electrodes 100 μm wide and spaced 400 μm apart (Fig. 5A). Patterning was effective for the range of microgel sizes, with larger microgels patterning more quickly than smaller ones, as predicted.[8] The alginate microgel pattern was maintained upon agarose gelation by brief immersion in ice–water (Fig. 5B). We then extended this technique to alginate microbeads containing dispersed BMEL cells, positioned into parallel lines within 1% agarose (Fig. 5C). Cell survival was high following DEP patterning for several minutes, agarose gelation by ice–water immersion, subsequent removal of the free-standing tissue, and transfer to a Petri dish for culture (Fig. 5C).

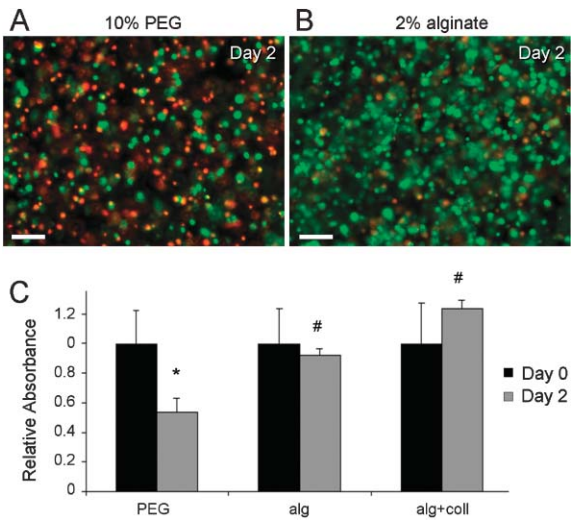

Fig. 4 Bipotential mouse embryonic liver (BMEL) cell survival improves in alginate over PEG hydrogels. (A,B) Viability of BMEL cells encapsulated in 10% 3.4 kDa PEG (A) and 2% alginate (B) was evaluated on day 2. Fluorescent labeling distinguished viable (green) from non-viable (red) cells. Scale bars: 100 μm. (C) BMEL survival was also assessed quantitatively by MTT assay on days 0 and 2 in 10% PEG, 2% alginate (alg), and 2% alginate with 0.2 mg mL^{-1} rat tail collagen (alg + coll). Absorbance measures are normalized to day 0 values. Data are mean ± SD (n = 5), and statistical significance is indicated by (*) for day 2 relative to day 0, and by (#) relative to PEG gels on day 2, with $p < 0.001$ (Student's *t*-test).

One concern with the multiphase approach is the potential for interactions between the polymer phases. For example, small polymer chains comprising a bulk phase may intercalate into a local-phase biomaterial with particularly large mesh size. To prevent such infiltration, microgels can be coated with a permeation barrier, for example *via* layer-by-layer deposition of poly-L-lysine (PLL). Multilayered alginate–PLL–alginate (APA) microspheres have been utilized extensively to immunoisolate encapsulated pancreatic islet cells, effectively preventing the passage of molecules as small as 10 kDa.[23,24] We verified this concept by embedding APA microspheres in agarose and found that the PLL layer effectively excluded agarose from the central alginate core. This was evidenced by solubilizing the alginate *via* exposure to sodium citrate; cells initially dispersed within the alginate microgel settled to the bottom of the void and aggregated (data not shown).

Conclusion

In this study, we extended a DEP-based method for 3D electropatterning of living cells within hydrogels to the patterning of pre-formed cellular microgels. This multiphase strategy effectively overcame a practical (but not theoretical) limitation of DEP electropatterning to low-conductivity and low-viscosity biomaterials with remotely-triggered gelation (*e.g.*, light or temperature). Segregation from the DEP-restricted bulk-phase hydrogel allows encapsulated cells to be surrounded by virtually any local-phase microgel biomaterial chosen to best support cell fate and function. Thus, while DEP-based methods for patterning of cells in 3D would be difficult in alginate due to its high conductivity, high viscosity, and ionic gelation, we were able to micropattern viable progenitor cells locally surrounded by alginate within a bulk agarose tissue. Because cell encapsulation has been explored extensively for cell transplantation and tissue engineering applications,[23,25,26] a plethora of methods exist to form

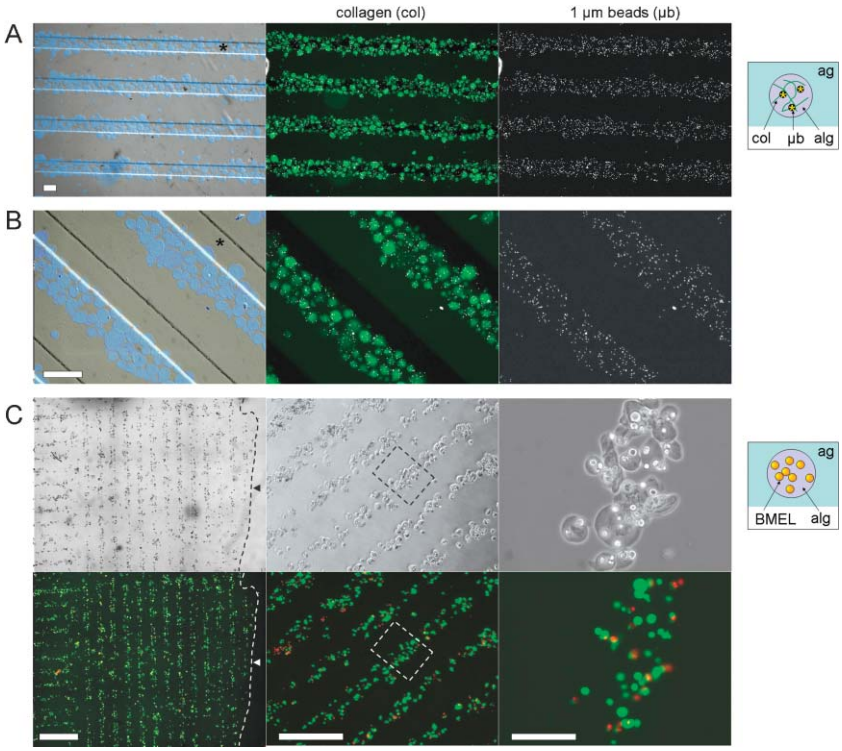

Fig. 5 Positive DEP patterning of alginate microgels within 250 μm thick agarose gels. (A, B) Alginate microgels containing embedded fluorescent collagen (green) and 1 μm diameter polystyrene microbeads (white) were electropatterned into a parallel line pattern within 1% agarose. Microgels (blue pseudocolor) localize to exposed ITO electrodes (*) within liquid agarose (A). The microgel pattern is maintained after agarose gelation (B); here, a spatially uniform hydrogel expansion (<1%) shifted the pattern ~100 μm from the electrodes (*). Scale bars: 100 μm. (C) Alginate microgels containing embedded BMEL cells are shown electropatterned in a parallel line pattern within a free-floating agarose slab after removal from the patterning chamber. The edge of the multiphase tissue is indicated by the arrowhead. Live/dead labeling performed 1 h following polymerization identifies viable (green) and non-viable (red) embedded BMEL cells. Scale bars: 1 mm (left), 500 μm (center), 100 μm (right). ag: 1% agarose gel, alg: 2% calcium alginate gel, col: collagen, μb: microbead, BMEL: bipotential mouse embryonic liver cell.

cell-laden microgels. For example, microspheres of many natural and synthetic hydrogels are routinely formed by emulsification or droplet extrusion,[21] whereas photopatterning or micromolding techniques can form complex microgel shapes.[18,19,27] Simple methods to assemble these tissue sub-units have been reported recently,[28] showing improved nutrient transport and scalability over homogeneous constructs. The multiphase, hierarchical approach to building inhomogeneous tissues is promising in its ability to tailor the local cell microenviroment separately from the bulk tissue, which likely has different mechanical, physical, and chemical requirements. In the future, precise 3D microorganization of these sub-units, by this layer-by-layer patterning method or others, may further improve the function of engineered tissues.

References

1 A. Khademhosseini, R. Langer, J. Borenstein and J. P. Vacanti, *Proc. Natl. Acad. Sci. U. S. A.*, 2006, **103**, 2480–2487.
2 S. R. Khetani and S. N. Bhatia, *Curr. Opin. Biotechnol.*, 2006, **17**, 524–531.
3 S. N. Bhatia, U. J. Balis, M. L. Yarmush and M. Toner, *FASEB J.*, 1999, **13**, 1883–1900.
4 R. McBeath, D. M. Pirone, C. M. Nelson, K. Bhadriraju and C. S. Chen, *Dev. Cell*, 2004, **6**, 483–495.
5 D. R. Albrecht, G. H. Underhill, T. B. Wassermann, R. L. Sah and S. N. Bhatia, *Nat. Methods*, 2006, **3**, 369–375.
6 T. M. Patz, A. Doraiswamy, R. J. Narayan, W. He, Y. Zhong, R. Bellamkonda, R. Modi and D. B. Chrisey, *J. Biomed. Mater. Res., Part B*, 2006, **78**, 124–130.
7 B. R. Ringeisen, C. M. Othon, J. A. Barron, D. Young and B. J. Spargo, *Biotechnol. J.*, 2006, **1**, 930–948.
8 D. R. Albrecht, R. L. Sah and S. N. Bhatia, *Biophys. J.*, 2004, **87**, 2131–2147.
9 G. H. Underhill, A. A. Chen, D. R. Albrecht and S. N. Bhatia, *Biomaterials*, 2007, **28**, 256–270.
10 H. J. Kong, M. K. Smith and D. J. Mooney, *Biomaterials*, 2003, **24**, 4023–4029.
11 K. A. Smeds, A. Pfister-Serres, D. Miki, K. Dastgheib, M. Inoue, D. L. Hatchell and M. W. Grinstaff, *J. Biomed. Mater. Res.*, 2001, **54**, 115–121.
12 J. H. Collier, B. H. Hu, J. W. Ruberti, J. Zhang, P. Shum, D. H. Thompson and P. B. Messersmith, *J. Am. Chem. Soc.*, 2001, **123**, 9463–9464.
13 G. Fuhr, H. Glasser, T. Muller and T. Schnelle, *Biochim. Biophys. Acta*, 1994, **1201**, 353–360.
14 T. B. Jones, *Electromechanics of particles*, Cambridge University Press, Cambridge, 1995.
15 J. Voldman, *Annu. Rev. Biomed. Eng.*, 2006, **8**, 425–454.
16 H. Strick-Marchand and M. C. Weiss, *Hepatology*, 2002, **36**, 794–804.
17 H. Strick-Marchand, S. Morosan, P. Charneau, D. Kremsdorf and M. C. Weiss, *Proc. Natl. Acad. Sci. U. S. A.*, 2004, **101**, 8360–8365.
18 D. R. Albrecht, V. L. Tsang, R. L. Sah and S. N. Bhatia, *Lab Chip*, 2005, **5**, 111–118.
19 V. A. Liu and S. N. Bhatia, *Biomed. Microdevices*, 2002, **4**, 257–266.
20 M. Peirone, C. J. Ross, G. Hortelano, J. L. Brash and P. L. Chang, *J. Biomed. Mater. Res.*, 1998, **42**, 587–596.
21 O. Smidsrod and G. Skjak-Braek, *Trends Biotechnol.*, 1990, **8**, 71–78.

22 S. J. Bryant and K. S. Anseth, *J. Biomed. Mater. Res.*, 2002, **59**, 63–72.
23 F. Lim and A. M. Sun, *Science*, 1980, **210**, 908–910.
24 R. Robitaille, F. A. Leblond, Y. Bourgeois, N. Henley, M. Loignon and J. P. Halle, *J. Biomed. Mater. Res.*, 2000, **50**, 420–427.
25 O. Hauser, E. Prieschl-Grassauer and B. Salmons, *Curr. Opin. Mol. Ther.*, 2004, **6**, 412–420.
26 S. M. Dang, S. Gerecht-Nir, J. Chen, J. Itskovitz-Eldor and P. W. Zandstra, *Stem Cells*, 2004, **22**, 275–282.
27 J. Yeh, Y. Ling, J. M. Karp, J. Gantz, A. Chandawarkar, G. Eng, J. Blumling 3rd, R. Langer and A. Khademhosseini, *Biomaterials*, 2006, **27**, 5391–5398.
28 A. P. McGuigan and M. V. Sefton, *Proc. Natl. Acad. Sci. U. S. A.*, 2006, **103**, 11461–11466.
29 Y. Huang, X. B. Wang, F. F. Becker and P. R. Gascoyne, *Biophys. J.*, 1997, **73**, 1118–1129.
30 M. Esch, V. L. Sukhorukov, M. Kurschner and U. Zimmermann, *Biopolymers*, 1999, **50**, 227–237.